Studies on the kinetics of oxidation of $Pu_yTh_{1-y}O_{2-x}$ ($y = 0.2, 0.3$ and 0.7) in air

S.K. Sali, S. Sampath, V. Venugopal *

Fuel Chemistry Division, Bhabha Atomic Research Centre, Trombay, Mumbai 400085, India

Abstract

Oxidation of sintered thorium–plutonium mixed oxide pellets was studied by thermogravimetry in the temperature range 400–1200 K. The kinetics of oxidation was found to be controlled by oxygen chemical diffusion with activation energies in the range 25–50 kJ mol^{-1}. Oxygen chemical diffusion coefficients are reported for $Pu_{0.3}Th_{0.7}O_{1.94}$. © 1998 Elsevier Science B.V.

1. Introduction

Oxide nuclear fuels undergo oxidation or reduction during fabrication, storage or chemical interaction with fission products or clad materials during reactor operation. Kinetics of oxidation of UO_{2+x}, (U, Pu)$O_{2\pm x}$, (U, Th)O_{2+x} and PuO_{2-x} have been studied in detail and are reported to be controlled by oxygen chemical diffusion [1–4]. Limited literature on this aspect is available on Th–Pu–O system. ThO_2 and PuO_2 were reported to form complete range of solid solution with fluorite structure, the lattice parameter varying from 0.5598 nm to 0.5396 nm [5]. Nuclear and material aspects of the thorium fuel cycle have been reviewed [6]. (Th, Pu)O_2 containing 2–4% PuO_2 is a possible candidate in advanced thermal reactor fuel concepts [7]. Fuel pellets of (Th, Pu)O_2 containing 18–35% PuO_2, typical of FBR fuel compositions have been fabricated for irradiation testing [8]. The present work is on the oxidation kinetic behaviour of sintered pellets of (Pu, Th)O_{2-x} with varying plutonium content.

2. Experimental

Sintered plutonium–thorium oxide pellets of compositions $Pu_yTh_{1-y}O_{2-x}$ ($y = 0.2, 0.3$ and 0.7) were obtained

---

* Corresponding author.

by solid state mixing, pelleting and sintering in hydrogen at 1873 K. Pellets weighing around 700 mg were of diameter 4 mm and length 6 mm. Oxidation kinetic studies were carried out in dry air using Mettler thermoanalyser with ±0.01 mg precision at a rate of heating of 4 K/min. The thermoanalyser was calibrated from the weight loss obtained for the decomposition of 100 mg of $CuSO_4 \cdot 5H_2O$ to CuO during heating to 1273 K. Calculated and experimental weight losses were in good agreement indicating reliability of the measurement.

3. Results and discussion

The fraction oxidised, α, against temperature (T) plots of the three compositions of (Pu$_y$Th$_{1-y}$)O_{2-x} are reproduced in Fig. 1. A, B and C refer to the compositions with $y = 0.7$, 0.3 and 0.2 respectively. The constant weight obtained at 1073 K during oxidation in air confirms the formation of the stoichiometric dioxide, $MO_{2.00}$ (M = Pu + Th). The oxygen to metal ratios (O/M) of the samples were calculated to be 1.8, 1.94 and 1.96 for $y = 0.7$, 0.3 and 0.2 respectively. With $y = 0.2$ and 0.3, oxidation is observed to be in a single step, $MO_{2-x} \rightarrow MO_{2.00}$. With $y = 0.7$, oxidation is found to take place in two steps, one rapidly at a low temperature of 400 K and the other in the temperature range 500–900 K. X-ray powder diffraction of the starting materials showed single phase fcc for $y = 0.2$ and 0.3. However mixed oxide with $y = 0.7$ was found to

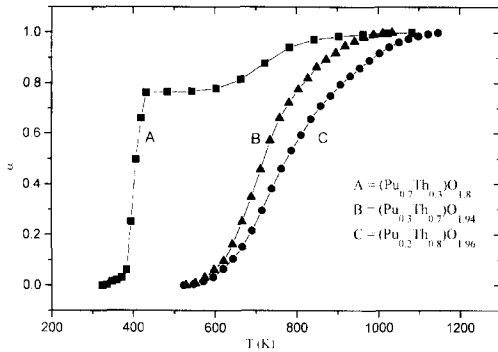Fig. 1. α against temperature plots for $Pu_xTh_{1-x}O_{2-x}$ in air.

be a mixture of M_2O_{3+x} and MO_{2-x}. This was in conformity with the low O/M of 1.8 obtained for the sample, suggesting a two phase mixture. Thorium dioxide, ThO_2, is the only compound in the thorium-oxygen system upto its melting point and exists as single cubic phase with fluorite structure whereas in the plutonium-oxygen system, a number of binary oxides are reported; $C-Pu_2O_3$ ($PuO_{1.52}$) and $C'-Pu_2O_3$ ($PuO_{1.62+x}$) both with bcc structure are obtained by the reduction of PuO_2 with hydrogen at high temperatures [9]. Hence it can be concluded that the two phase mixture in $Pu_{0.7}Th_{0.3}O_{1.8}$ consists of MO_{2-x} phase rich in thorium and M_2O_{3+x} phase rich in plutonium.

The kinetics of oxidation of mixed oxide was determined by the method suggested by Zsako [10] using a computer program. The basic equation used by Zsako can be represented by

$$\ln g(\alpha) - \ln p(x) = \ln[ZE/qR], \qquad (1)$$

where $g(\alpha) = \int d\alpha/f(\alpha) = kt$, $f(\alpha)$ is a function of α, fraction reacted and $p(x)$ is a function of x defined as $x = E/RT$. Z, E, R, q and T are, respectively, the pre-exponential factor of the Arrhenius equation, activation energy, gas constant, the heating rate and absolute temperature. As $\ln[ZE/qR]$ is constant for a given reaction at a constant heating rate, the plot of $\ln g(\alpha)$ against T and $\ln p(x)$ with T should have the same slope provided the assumed mechanism for calculation of $g(\alpha)$ and the assumed activation energy for calculation of $p(x)$ are correct.

The program first calculates the approximate value of the activation energy by the method of Piloyan and Novikova [11] using only TG data. Values were taken on either side of the approximate value of the activation energy to facilitate iteration with respect to E. The standard deviation of the difference of $\ln g(\alpha)$ and $\ln p(x)$ was calculated for a particular assumed reaction mechanism in the temperature range of interest and for each assumed activation energy. The likely mechanism is the one for which the standard deviation is minimum for a particular combination of activation energy and reaction mechanism. Typical computer outputs containing standard deviations for various mechanisms and activation energies for oxidation of $Pu_{0.3}Th_{0.7}O_{1.94}$ and $Pu_{0.2}Th_{0.8}O_{1.96}$ are

Table 1
Oxidation of $Pu_{0.3}Th_{0.7}O_{1.94}$ in air: A typical computer output (standard deviation) to find the best fit among the different reaction mechanisms

Mechanisms $g(\alpha)$	Input activation energies (kJ/mol)						
	30	38	47	55	64	72	80
$\alpha^{1/4}$	0.5361	0.6756	0.8144	0.9526	1.0900	1.2280	1.3650
$\alpha^{1/3}$	0.4929	0.6321	0.7707	0.9087	1.0460	1.1840	1.3210
$\alpha^{1/2}$	0.4091	0.5467	0.6843	0.8218	0.9592	1.0960	1.2330
α	0.2126	0.3187	0.4431	0.5737	0.7068	0.8412	0.9763
$\alpha^{3/2}$	0.2833	0.2479	0.2856	0.3741	0.4862	0.6086	0.7363
α^2	0.5220	0.4225	0.3521	0.3287	0.3609	0.4364	0.5369
$1-(1-\alpha)^{1/3}$	0.1570	0.1791	0.2797	0.4032	0.5336	0.6668	0.8013
$1-(1-\alpha)^{1/2}$	0.1569	0.2137	0.3246	0.4508	0.5821	0.7157	0.8503
$1-\ln(1-\alpha)^{1/4}$	0.4649	0.6045	0.7433	0.8816	1.0190	0.8169	0.9288
$-\ln(1-\alpha)^{1/3}$	0.3980	0.5372	0.6758	0.8139	0.9517	1.0890	1.2270
$-\ln(1-\alpha)^{1/2}$	0.2677	0.4045	0.5419	0.6794	0.8168	0.9540	1.0910
$-\ln(1-\alpha)^{2/3}$	0.1524	0.2773	0.4111	0.5469	0.6833	0.8199	0.9566
$-\ln(1-\alpha)$	0.2029	**0.1354**	0.1855	0.2980	0.4256	0.5579	0.6921
$(1-\alpha)\ln(1-\alpha)+\alpha$	0.6426	0.5259	0.4242	0.3495	0.3204	0.3480	0.4212
$1-2\alpha/3-(1-\alpha)^{2/3}$	0.6963	0.5747	0.4642	0.3737	0.3197	0.3205	0.3757
$[1-(1-\alpha)^{1/3}]^2$	0.8112	0.6828	0.5607	0.4490	0.3569	0.3020	0.3048
$[(1+\alpha)^{1/3}-1]^2$	0.4223	0.3438	0.3119	0.3388	0.4128	0.5137	0.6285
$1-(1-\alpha)^2$	0.3493	0.4775	0.6100	0.7442	0.8793	1.0150	1.1510
$1-(1-\alpha)^3$	0.4422	0.5763	0.7117	0.8476	0.9838	1.1200	1.2570
$1-(1-\alpha)^4$	0.5028	0.6394	0.7762	0.9131	1.0500	1.1870	1.3240

Table 2
Oxidation of $Pu_{0.2}Th_{0.8}O_{1.96}$ in air: A typical computer output (standard deviation) to find the best fit among the different reaction mechanisms

Mechanisms $g(\alpha)$	Input activation energies (kJ/mol)						
	16	25	33	42	50	58	67
$\alpha^{1/4}$	0.3022	0.4192	0.5339	0.6474	0.7602	0.8725	0.9844
$\alpha^{1/3}$	0.2801	0.3970	0.5117	0.6252	0.7379	0.8502	0.9621
$\alpha^{1/2}$	0.2365	0.3530	0.4675	0.5808	0.6935	0.8057	0.9176
α	0.1155	0.2248	0.3371	0.4494	0.5614	0.6732	0.7848
$\alpha^{3/2}$	0.0910	0.1183	0.2150	0.3225	0.4324	0.5429	0.6537
α^2	0.2019	0.1224	0.1278	0.2088	0.3102	0.4170	0.5257
$1-(1-\alpha)^{1/3}$	0.0586	0.0945	0.2023	0.3139	0.4258	0.5375	0.6491
$1-(1-\alpha)^{1/2}$	0.0510	0.1308	0.2407	0.3525	0.4644	0.5761	0.6877
$-\ln(1-\alpha)^{1/4}$	0.2464	0.3635	0.4783	0.5918	0.7046	0.8169	0.9288
$-\ln(1-\alpha)^{1/3}$	0.2058	0.3228	0.4375	0.5510	0.6638	0.7760	0.8880
$-\ln(1-\alpha)^{1/2}$	0.1251	0.2415	0.3560	0.4695	0.5822	0.6944	0.8063
$-\ln(1-\alpha)^{2/3}$	0.4886	0.1609	0.2749	0.3881	0.5007	0.6128	0.7247
$-\ln(1-\alpha)$	0.1271	**0.0365**	0.1159	0.2266	0.3384	0.4502	0.5618
$(1-\alpha)\ln(1-\alpha)+\alpha$	0.3016	0.1964	0.1175	0.1234	0.2054	0.3071	0.4139
$1-2\alpha/3-(1-\alpha)^{2/3}$	0.3485	0.2388	0.1432	0.1016	0.1603	0.2575	0.3631
$[1-(1-\alpha)^{1/3}-1]^2$	0.4482	0.3342	0.2256	0.1294	0.0912	0.1588	0.2592
$[(1+\alpha)^{1/3}-1]^2$	0.1382	0.1051	0.1725	0.2724	0.3793	0.4884	0.5983
$1-(1-\alpha)^2$	0.2320	0.3470	0.4608	0.5737	0.6861	0.7981	0.9098
$1-(1-\alpha)^3$	0.2948	0.4111	0.5255	0.6387	0.7513	0.8634	0.9753
$1-(1-\alpha)^4$	0.3279	0.4447	0.5593	0.6727	0.7854	0.8976	1.0100

given in Tables 1 and 2 respectively. They show that the lowest standard deviation occurs at activation energies of 38 kJ mol^{-1} and 25 kJ mol^{-1} respectively for $g(\alpha)=-\ln(1-\alpha)$. Further iteration with smaller intervals of activation energy gives E values of 39.4 kJ mol^{-1} and $Z=3.17\times10^{-1}$ s^{-1} for $Pu_{0.3}Th_{0.7}O_{1.94}$ and E of 25.2 kJ mol^{-1} and $Z=1.65\times10^{-2}$ s^{-1} for $Pu_{0.2}Th_{0.8}O_{1.96}$. Oxidation of $Pu_{0.7}Th_{0.3}O_{1.8}$ samples however followed two mechanisms for the kinetics corresponding to two steps in the α vs. T curve. The first step gave a mechanism of nucleation and growth with $g(\alpha)=-[\ln(1-\alpha)]^{1/4}$ and the second step, diffusion controlled mechanism with $g(\alpha)=-\ln(1-\alpha)$. The reaction kinetics observed suggest that the oxidation of $(Th, Pu)O_{2-x}$ to $(Th, Pu)O_{2.00}$ is

a diffusion — controlled process similar to $(Th, U)O_{2+x}$, UO_{2+x} and PuO_{2-x} and $(U, Pu)O_{2\pm x}$ [1–4].

With $y=0.2$ and 0.3 in $Pu_yTh_{1-y}O_{2-x}$, the oxidation involves no discrete product layer. The surface of MO_{2-x} is rapidly equilibrated to $MO_{2.00}$ by oxygen and oxidation kinetics is controlled by diffusion of oxygen from the surface to the interior. However for $y=0.7$, which consists of two phases, M_2O_{3+x} phase rich in plutonium and MO_{2-x} phase rich in thorium, oxidation proceeds in two steps; (i) oxidation of M_2O_{3+x} to MO_{2-x} above 400 K and (ii) oxidation of MO_{2-x} to MO_2 in the temperature range 500–900 K. The second step is similar to the oxidation of mixed oxide with $y=0.2$ and 0.3. However, for the first step the mechanism of kinetics is different as

Table 3
Oxygen chemical diffusion data in actinide oxides

| Oxide	E (kJ/mol)	$\log D$ (m² s⁻¹)	Temp. range (K)	Reference
$PuO_{1.97}$	50.8	$(-2.4\times10^3/T)-6.1$	1000–1200	Bayoglu [1]
$(U, Pu)O_{1.98}$	52.9	$(-2.7\times10^3/T)-6.47$	625–1000	Bayoglu [1]
$U_{0.7}Pu_{0.3}O_{2-x}$	50.4	–	700–1300	Sampath [2]
$Th_{0.8}Pu_{0.2}O_{1.96}$	25.2	–	700–1300	present work
$Th_{0.7}Pu_{0.3}O_{1.94}$	48.6	$(-2.5\times10^3/T)-5.79$	700–1300	present work
$Th_{0.6}U_{0.4}O_{2+x}$	66.8	$(-3.49\times10^3/T)-7.83$	1282–1373	Matsui [4]
$Th_{0.8}U_{0.2}O_{2+x}$	93.1	$(-4.8\times10^3/T)-6.2$	1282–1373	Matsui [4]
$Pu_{0.2}U_{0.8}O_{2+x}$	72.4	$(-3.78\times10^3/T)-6.18$	1173–1823	Sari [3]
UO_{2+x}	89.5	$(-4.68\times10^3/T)-5.74$	873–1273	Bayoglu [1]
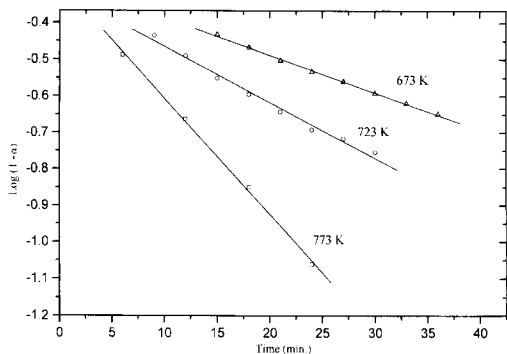
Fig. 2. Log$(1 - \alpha)$ against time plots for $Pu_{0.3}Th_{0.7}O_{1.94}$.

Fig. 3. Log D against $1/T$ plot for $Pu_{0.3}Th_{0.7}O_{1.94}$.

the product layer is discrete from the reactant and the kinetics is controlled by nucleation and growth of second phase.

Oxygen chemical diffusion coefficient data were obtained by isothermal kinetics for the composition $Pu_{0.3}Th_{0.7}O_{1.94}$ using the expression given by Matsui and Naito [4]:

$$\log(1 - \alpha) = -0.252 - 1/2.303\left[(2.405)^2/a^2\right.$$
$$\left. + 2/(4b^2)\right]Dt, \qquad (2)$$

where $2a$ and $2b$ are respectively sample diameter and sample thickness in meters and t is time in seconds. The pellets used were of diameter 4 mm and thickness 6 mm. Isothermal kinetics was carried out at 673, 723 and 773 K and plots of log$(1 - \alpha)$ against time for the three temperatures are given in Fig. 2. The chemical diffusion coefficients (D) obtained were 2.82×10^{-10} m^2/s at 673 K, 4.26×10^{-10} m^2/s at 723 K and 7.6×10^{-10} m^2/s at 773 K. Fig. 3 plots log D versus $1/T$; activation energy obtained from the slope was 48.6 kJ mol^{-1}.

Oxygen chemical diffusion data on the actinide oxides reported in literature and in the present work is given in Table 3. A comparison of reported activation energies for the oxidation of hypo- and hyper stoichiometric actinide oxides, AO_{2-x} and AO_{2+x}($A =$ U, Pu, U + Pu, U + Th or Th + Pu) shows that they are in the range 25–50 kJ mol^{-1} for AO_{2-x} and 65–95 kJ mol^{-1} for AO_{2+x} [1–4]. From this, one can conclude that AO_{2-x} oxidation, which involves anion vacancy migration, is associated with lower activation energies as compared to AO_{2+x} oxidation, which involves anion interstitialcy mechanism and consequently associated with higher activation energies. This is sup-
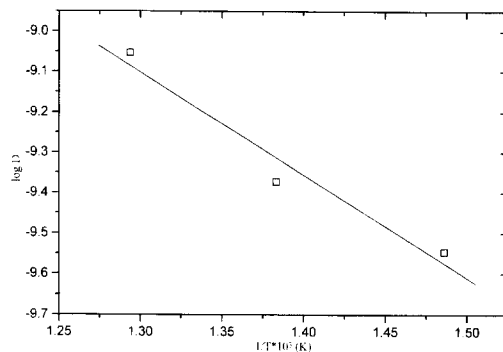
ported by theoretical studies of point defect properties of uranium dioxide, reported by Catlow and Lidiard [12].

References

[1] A.S. Bayoglu, R. Lorenzelli, Solid State Ionics 12 (1994) 53.
[2] S. Sampath, R.G. Hadap, R.K. Swamy, D.M. Chackraburtty, Thermochim. Acta 32 (1979) 326.
[3] C. Sari, J. Nucl. Mater. 78 (1978) 425.
[4] T. Matsui, K. Naito, J. Nucl. Mater. 135 (1985) 149.
[5] R.N.R. Mulford, F.H. Ellinger, J. Phys. Chem. 62 (1958) 1466.
[6] P. Rodriguez, C.V. Sundaram, J. Nucl. Mater. 100 (1981) 227.
[7] K. Balkrishnan, C. Ganguly, Mater. Sci. Forum 48&49 (1989) 125.
[8] D.E. Ramussen, M.W. Benecke, W.R. Jentzin, R.B. Mccord, Trans. Am. Nucl. Soc. 32 (1979) 246.
[9] C. Keller, in: J.C. Bailor, Jr, H.J. Emeleus, Sir R. Nyholm, A.F. Trotman-Dickenson (Eds.), Comprehensive Inorganic Chemistry, vol. 5, Pergamon, 1973, p. 219.
[10] J. Zsako, J. Phys. Chem. 72 (1968) 2406.
[11] G.O. Piloyan, O.S. Novikova, Russ. J. Inorg. Chem. 12 (1967) 313.
[12] C.R.A. Catlow, A.B. Lidiard, Thermodyn. Nucl. Mater., vol. 2 IAEA, 1975, p. 27.